

MANIPULATING MEMBRANE HYDROPHOBICITY BY INTEGRATING POLYETHYLENE-COATED FUME SILICA IN PVDF MEMBRANE

Pei Thing Chang^a, Sarveswaran Paranthaman^a, Aishah Rosli^b, Siew Chun Low^{a*}

^aSchool of Chemical Engineering, Universiti Sains Malaysia, Engineering Campus, 14300, Nibong Tebal, Penang, Malaysia

^bSchool of Chemical and Energy Engineering, Faculty of Engineering, Universiti Teknologi Malaysia, 81310 UTM Johor Bahru, Johor, Malaysia

Article history

Received

11 July 2021

Received in revised form

24 September 2021

Accepted

10 October 2021

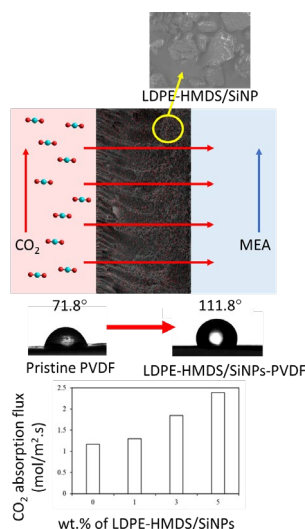
Published online

28 February 2022

*Corresponding author

chsclo@usm.my

Graphical abstract



Abstract

Membrane gas absorption (MGA) as an emerging technology exhibits superior advantages in comparison to conventional carbon dioxide (CO₂) absorption processes. However, the decrease in membrane flux, induced by membrane wetting is a significant issue to be pondered upon. Thus, fabrication of an anti-wetting composite membrane is essential to retain and sustain the MGA performance. In this work, silica nanoparticles (SiNPs) is first coated with hydrophobic low-density polyethylene (LDPE). Then, integrating LDPE-HMDS/SiNPs fillers into the polyvinylidene fluoride (PVDF) matrix to increase its hydrophobicity. The incorporation of LDPE-coated silica into PVDF polymer enhanced the contact angle values from 71.8° to 111.8°, indicates the improvement of membrane anti-wetting ability. Despite the similar finger-like layer laid on top of the sponge-like structure for pristine and composite membranes, the incorporation of LDPE-HMDS/SiNPs has reduced in the length ratio of finger-like to sponge-like layer. The changed in the membrane morphology induced higher membrane hydrophobicity which prevent membrane from getting wet easily especially in long term of operation. In addition, EDX surface mapping and lining profiles clearly proved that the LDPE-HMDS/SiNPs were distributed evenly in the composite membranes indicates the good interfacial compatibility between PVDF polymer and LDPE-coated silica. In term of CO₂ absorption flux, the embedment of LDPE-HMDS/SiNPs in PVDF polymer matrix demonstrated 2.4x10⁻³ mol/m².s which was 2 times higher than that of the pristine membrane. This means the incorporation of LDPE-HMDS/SiNPs into the PVDF membrane has still played a pivotal role in overcoming membrane wetting drawbacks when in contact with the liquid absorbents.

Keywords: CO₂ removal, hydrophobic, LDPE, membrane gas absorption, silica coating

© 2022 Penerbit UTM Press. All rights reserved

1.0 INTRODUCTION

Carbon dioxide (CO₂) is widely known as the heat-trapping greenhouse gas. The increase in CO₂ emissions from anthropogenic sources, mainly from the burning of fossil fuels, accelerates the level of CO₂ in the earth's atmosphere, which then causes climate change that is likely to threaten life on earth [1]. Solvent absorption is one of the promising CO₂ capture technologies that has been widely used in industry particularly the power industries, but it also encounters several shortcomings in the absorption column, such as large footprint, high cost, and inevitable operational problems [2,3]. Membrane gas absorption (MGA) has emerged as an

alternative technology for CO₂ removal to address these issues, combining the benefits of solvent absorption and membrane separation technologies [4].

MGA provides a smaller footprint, a larger contact area per unit volume, and can control the flowrate of gas and liquid independently to solve operational problems such as flooding, liquid channeling, foaming, and entrainment faced by the absorption column [2,5]. For example, Kvaerner Process Systems (KPS) has cooperated with W.L. Gore & Associates GmbH (GORE), SGL Carbon Group (SGL) and Ottestad Breathing Systems (OBS) to develop a MGA pilot plant for CO₂ removal in Norway in 1992. The pilot plant showed a CO₂ capture efficiency of 85% during operation and an exhaust gas flow rate

of 2610 kg/h [6]. In addition, the Gas Technology Institute (GTI) in United State also successfully developed a MGA technology for CO₂ reduction in 2010, called Carbo-Lock™. The CO₂ capture efficiency reaches more than 90% within 120 hours of operation [7].

However, the implementation of the MGA process also faces challenges such as the selection of absorption solvents, the selection of the module type, and the high operating cost due to the wetting tendency of the membrane during operation. Among these concerns, wetting is the focus of current work. Wetting is one of the inevitable shortcomings of MGA due to the penetration of liquid absorbent into the pores of the membrane during long-term operation. This phenomenon leads to a significant dropped in CO₂ absorption flux [8]. Even if the liquid absorbent penetrates only 2% of the membrane pores [9], the membrane mass transfer resistance can still be increased to 60%, resulting in a significant drop in the flux of CO₂ absorption. In terms of economic analysis, membrane wetting issue have a great impact on MGA operating expenses. Membranes that are easily wetted (short lifespan) require frequent membrane replacement, resulting in high operating and maintaining costs [10].

To overcome this challenge, the priority of membrane selection is on hydrophobic membranes, includes polyvinylidene (PVDF), polytetrafluoroethylene (PTFE), and polypropylene (PP) [11,12]. PVDF has better advantages than PTFE and PP, such as cheaper and higher porosity that reduces membrane resistance. While among these membranes, PTFE has the highest hydrophobicity, but it cannot dissolve in common organic solvents that can dissolve PVDF. PVDF will be the preferred choice for this reason [13,14]. However, the intrinsic hydrophobicity of PVDF is not sufficient for long-term operation because it still suffers from severe wetting problems. Therefore, the membrane must be modified to increase the hydrophobicity of the membrane, thereby improving the wetting resistance [14].

At present, several techniques including plasma treatment [15], electrospinning [16] and blending of polymer solution with inorganic fillers [9] have been studied to change the properties and structure of the membrane to improve its hydrophobicity. Among these methods, blending polymer solutions with inorganic fillers is always the prior option. This is because mixed matrix membranes (MMM) with inorganic fillers embedded into the polymer matrix is a well-established and simple method to improve the membrane hydrophobicity. In a polymer matrix, the dispersed inorganic fillers will alter the morphology and porosity of the membrane. Thereby increasing the surface roughness and improving the membrane hydrophobicity [17]. Due to its well-defined structure and cost-effectiveness, inorganic fillers (such as hydrophobic SiNPs) have been widely chosen by researchers to synthesize hydrophobic MMM [18]. For instance, Sun *et al.*, (2017) incorporated hydrophobic silica nanoparticles into the membrane matrix to enhance the membrane hydrophobicity and proved that its water contact angle increased to 160° [19]. In the work of Toh *et al.*, (2020) by blending hydrophobic silica nanoparticles into the membrane matrix, a superhydrophobic membrane with a water contact angle as high as 151° was successfully produced [4]. The polydimethylsiloxane-SiO₂/PVDF-HFP MMM still exhibits a stable CO₂ absorption flux after being immersed in 2 M monoethanolamide (MEA) for 12 days. The CO₂ absorption flux was only slightly reduced from 1.18×10⁻² mol/m².s (initial

CO₂ absorption flux) to 0.97×10⁻² mol/m².s (after 12 days). Meanwhile, the surface modification of the nanoparticles helps to disperse the nanoparticles in the membrane matrix. Subsequently, optimize the membrane performance. As demonstrated by Rosli *et al.*, (2019) low-density polyethylene (LDPE) is a good linker for bridging membrane and nanoparticles [17]. The LDPE-modified nanoparticles were well distributed in the membrane matrix, which increases the hydrophobicity of the membrane. In the study, the CO₂ absorption flux of MMM during MGA operation was increased nearly three times when compared to the pristine PVDF membrane found at 2.0×10⁻⁴ mol/m².s.

In this study, hexamethyldisilazane/silica nanoparticles (HMDS/SiNPs) were surface modified with LDPE (denoted as LDPE-HMDS/SiNPs). Then, under a series of concentrations, it is incorporated into the PVDF membrane and is expected to improve the resistance to wetting during the MGA process. Dynamic light scattering (DLS) and thermogravimetric analysis (TGA) characterize the average hydrodynamic diameter of the LDPE-HMDS/SiNPs. The synergistic effect on the membrane properties can be observed through the changes of membrane morphology and contact angle.

2.0 METHODOLOGY

2.1 Materials

PVDF powder (Solvay Solexis), N-methyl-2-pyrrolidone (NMP, Sigma-Aldrich), and ethanol (ACS, ISO, Reag. Ph Eur, Merck) were used to fabricate the PVDF membrane. Hydrophobic fumed silica nanoparticles (HMDS/SiNPs or known as TS-530) were provided courtesy of Cabot (USA). LDPE and xylene supplied from Petline Sdn. Bhd (Malaysia) and Sigma-Aldrich (Germany), respectively, were used to prepare a coating solution to functionalize silica nanoparticles. Monoethanolamine (MEA) with purity 99% was purchased from Merck (Germany). It was diluted with deionized water to prepared 1M liquid absorbent in the MGA process. All the chemicals used were analytical grade.

2.2 HMDS/SiNPs Coated With LDPE

A mixed solution consisting of 5:1 v/v acetone and ethanol was prepared at 100 mL. Silica nanoparticles (5g, HMDS-SiNPs, TS-530) was added to the prepared mixture solution and agitated for 10 minutes. Meanwhile, 4 g of LDPE was dissolved in 100 mL of xylene solvent and stirred for 2 hours in a double jacket heating tank at 85°. Then, the heated solution was cooled to 75° and used as a coating solution for the functionalization of HMDS/SiNPs. The SiNPs was coated by mixing the suspended SiNPs with the LDPE coating solution, and then continuously stirred for 10 minutes. Finally, the coated LDPE-HMDS/SiNPs were filtered and air-dried under ambient condition [9].

2.3 LDPE-HMDS/SiNPs Characterization

Sizes of LDPE-coated HMDS/SiNPs were analyzed through dynamic light scattering (DLS) using Zetasizer Nano ZS900 (Malvern Instrument, UK). The hydrodynamic diameter of the nanoparticles suspended in water was continuously recorded

for 30 minutes. It is to observe the stability of the hydrodynamic diameter and its aggregation tendency.

Thermogravimetric analysis (TGA) was used to analyze the thermal decomposition of the membrane samples by Perkin Elmer (TGA7, USA). Weight loss of the sample was recorded from 50°C to 800°C in an inert N₂ atmosphere.

The chemical properties and functional groups of HMDS/SiNPs and LDPE-HMDS/SiNPs were characterized using Thermo Scientific Fourier transform infrared spectrometer (FTIR, Nicolet iS10, USA). The spectra was acquired from 32 scans using diamond crystal in the wavenumber range of 4000–400 cm⁻¹ with a resolution of 4 cm⁻¹.

2.4 Membrane Synthesis

Membrane was synthesized by a non-solvent induced phase separation (NIPS) process. Before dissolving the PVDF powder, the NMP solvent was heated to 40°C. 15% of the PVDF powder was added slowly into the solvent and stirred at 60 °C for 6 hours. The dope solution was allowed to cool to room temperature, and followed by 1 hour of sonication to eliminate air bubbles in the solution. Then, the polymer dope was casted on a glass plate with a thickness of 400 μm using a thin film applicator. Subsequently, immersed in a coagulation bath with ethanol and water composed of 20:80 for 24 hours. Finally, the pristine PVDF membrane was removed from the glass plate and washed with distilled water. The membrane was air-dried at room temperature for 3 days before carrying out the characterization and MGA test.

The composite membrane of PVDF/LDPE-HMDS/SiNPs was synthesized using a blending method. A specific amount of LDPE-HMDS/SiNPs (i.e. 1, 3, and 5 wt.%) relative to 15 wt.% of PVDF was incorporated into the NMP solvent. The solution was stirred for 30 minutes, and then sonicated for 30 minutes to better disperse the LDPE-HMDS/SiNPs. Then, slowly added PVDF powder into the suspended LDPE-HMDS/SiNPs/NMP solution at 60°C. Solution was continuously stirred for 24 hours to ensure homogeneous dispersion of nanoparticles. Finally, the polymer dope was cast in the same manner as the pristine membrane, as described above.

2.5 Membrane Characterization

The fabricated membranes were characterized to determine their chemical and physical properties. The static water contact angle of the membrane surface was measured by a goniometer (Rame-Hart 250 F-1, USA) to examine the hydrophobicity of the membrane. The direct measurement of the contact angle was based on the sessile drop of the micro-syringe on different areas of the membrane. The average value was recorded.

The surface and cross-sectional structure of the membranes were observed by a field emission scanning electron microscope (FESEM, SUPRA TM 35vp Zeiss, Germany). All the membranes were fractured in liquid nitrogen and then sputtered with a thin gold film to improve electrical conductivity. The images of the membrane were taken at an acceleration voltage of 3kV and magnification of 1000x and 2500x magnification. Besides, the composition of Si element on the membrane was analyzed by the energy-dispersive X-ray spectroscopy (EDX). The EDX lining and mapping were analyzed to detect Si dispersion.

2.6 MGA Performance

The experiments were conducted at atmospheric pressure and room temperature using the MGA set-up shown in Figure 1. Pure CO₂ was used as the feed gas, while MEA was used as a liquid absorbent. The gas and liquid were controlled at a flow rate of 100 mL/min. Before evaluating the separation performance, the system was ran for 15 minutes to achieve a steady-state. The CO₂ absorption flux, J_{CO_2} (mol/m².s), was calculated using Equation 1, where the inlet and retentate gas flow rates were measured by a bubble soap meter for a long-term MGA process of 30 hours [4].

$$J_{CO_2} = \frac{(Q_{g,i} - Q_{g,r})\rho_g}{MW_g A} \quad (1)$$

$Q_{g,i}$ is the inlet gas flow rate (mL/min), $Q_{g,r}$ is the retentate gas flow rate (mL/min), ρ_g is the density of CO₂ (g/mol), MW_g is the molecular weight of CO₂ and A is the membrane contacting area (m²).

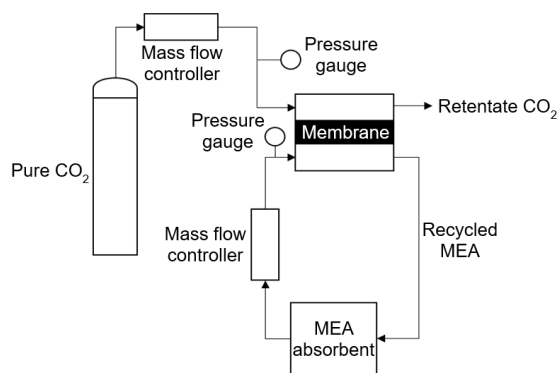


Figure 1 Schematic of MGA process

3.0 RESULTS AND DISCUSSION

3.1 Analysis Of HMDS/SiNPs Coated With LDPE

Modifying the membrane morphology will affect its hydrophobicity. Subsequently, it will control the performance of the membrane's wettability in the MGA. In this work, HMDS/SiNPs (TS-530) is first coated with LDPE and then incorporated into the polymer matrix of PVDF. It may anticipate that the resulting composite membrane will improve the polymer's wetting resistance due to the hydrophobicity of LDPE-HMDS/SiNPs. Figure 2 describes the overall functionalization process. The chemical structure of the silica has containing groups of silanol (Si-OH) makes it hydrophilic. The -OH groups, which form hydrogen bonds between two adjacent particles, lead to strong aggregates. It can cause dispersion problems by adding these hydrophilic Si-OH to the polymer matrix because the polymer-silica interaction is weaker than the interparticle forces [20]. As a result, it forms a defective composite membrane. Therefore, chemical modification is essentially required to modify the hydrophilicity of silica to hydrophobicity.

The original Si-OH has modified with hydrophobic hexamethyldisilazane (HMDS) organosilicon (Figure 2a) by Cabot Corporation. The silica -OH group has been replaced by

the methyl (–CH₃) group of HMDS organosilicon through a chemical reaction. Generally, C–H bonds are effective non-polar covalent bonds with hydrophobic properties [21,22]. By substituting the surface –OH groups on silica with –CH₃ groups, it will indirectly alter the initial hydrophilic SiNPs to a more pronounced hydrophobicity. The formation of an oxane bond with HMDS organosilane can eliminate the hydrogen of the hydroxyl group. The efficacy of enhancing the hydrophobicity of silica is not only by substituting the hydroxyl groups as the water adsorption sites. It can also be providing anchor points for the non-polar organic substitution of silanes. Thereby, it shields the polar substrates from interacting with water. The SEM image of HMDS-SiNPs shown in Figure 2a illustrates irregular shapes with rough surfaces. This may be due to the larger polymer size of HMDS polymers wrapped on the surface of silica.

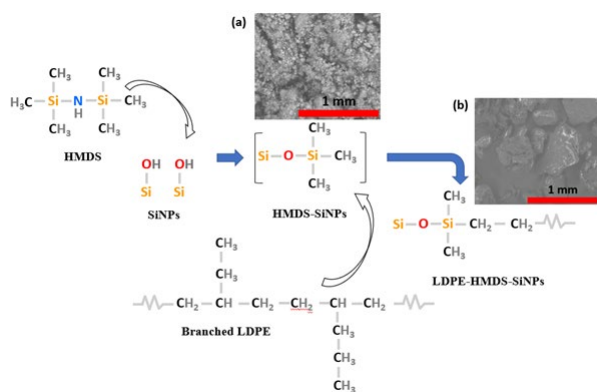


Figure 2 Chemical interaction pathways of silica nanoparticles (SiNPs) with hexamethyldisilazane (HMDS) and low-density polyethylene (LDPE)

In this work, HMDS/SiNPs is further coated with LDPE, to increase the organic-inorganic compatibility between HMDS, SiNPs and organic PVDF polymer. As shown in Figure 2b, LDPE can be linked covalently with the Si–O–Si and –CH₃ of HMDS/SiNPs to LDPE-HMDS/SiNPs. LDPE consists of long alkane chain, which is also known as a hydrophobic chain. The longer the hydrophobic chain, the higher the hydrophobicity. Therefore, surface coating of LDPE on HMDS/SiNPs causes additional long hydrophobic groups on the nanoparticles. It can indirectly augment the hydrophobicity of PVDF composite membrane to produce a wet-resistant membrane. In SEM image of Figure 2b, it detects a significant change of physical appearance of HMDS/SiNPs after surface-coated with LDPE. It shows a smoother surface of nanoparticles, which indicates the successful surface coating of HMDS/SiNPs with LDPE.

The DLS in Figure 3a demonstrates the successful coating of LDPE on HMDS/SiNPs. After LDPE coating, the hydrodynamic size of HMDS/SiNPs increased from 148.3 nm to 211.2 nm. It may be due to the functional group bonding of silica and LDPE (CH₂), resulting in larger particle size. Although fluctuation and increase in size were observed (Figure 3a), experiments showed a stable hydrodynamic size of LDPE-HMDS/SiNPs over the 30 mins of measurement. Although it is not able to attain a completely uniform distribution of the nanoparticles, the increased hydrophobicity of SiNPs due to the prevalence of

LDPE may be beneficial for a good interface between the nanoparticles and the PVDF membrane.

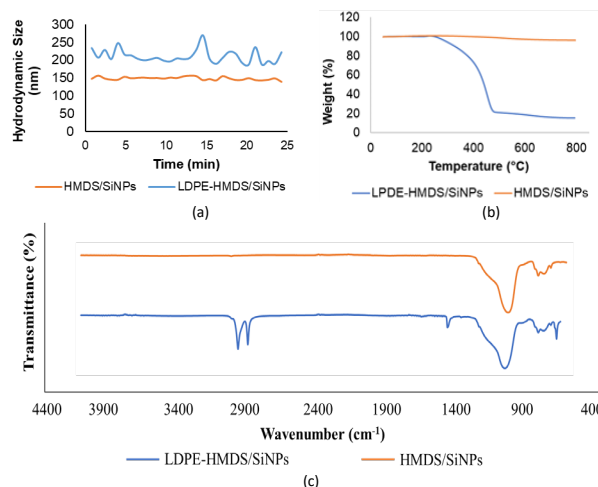


Figure 3 (a) Hydrodynamic size, (b) TGA curves profile and (c) FTIR spectrum of HMDS/SiNPs and LDPE-HMDS/SiNPs

It is also worth making sure that LDPE is well attached to HMDS/SiNPs, not just the possible partial coating. The thermogravimetric analysis in Figure 3b established further verification. HMDS/SiNPs and LDPE-HMDS/SiNPs are heated at elevated temperatures from 60°C to 800°C while monitoring the changing mass to obtain the decomposition curve. The LDPE-coating can determine by the weight loss of LDPE-HMDS/SiNPs between 290°C and 490°C, at which the weight has significantly reduced. The mass loss indicates that at 290°C, LDPE begins to decompose and decompose completely beyond 490°C. However, the continuous heating up to 800°C did not degrade the LDPE-HMDS/SiNPs. Therefore, the remaining weight of LDPE-HMDS/SiNPs can denote as SiNPs weight. According to the decomposition curve of LDPE-HMDS/SiNPs (Figure 3b, blue line), approximately 78% of the mass loss occurs between 290°C to 490°C. It indicates the complete decomposition of LDPE and proves that the coating of LDPE on SiNPs is undeniable.

In addition, the FTIR spectrum shown in Figure 3c confirms the LDPE coating on HMDS/SiNPs. As shown in the figure, the chemical properties of HMDS/SiNPs have changed after the LDPE coating process. By comparing the spectra of HMDS/SiNPs and LDPE-HMDS/SiNPs, both showed a strong absorption peak near 1072 cm⁻¹. This peak is corresponded to the Si–O–Si asymmetric stretching vibration and also reflects the existence of silica. After the LDPE coating process, two new peaks are shown at 2900 cm⁻¹ and 2915 cm⁻¹ (Figure 3c, blue line). The presence of these peaks indicates the symmetric and asymmetric stretching vibration of –CH₂ from LDPE. This result verified that LDPE was successfully coated on HMDS/SiNPs.

3.2 Membrane Morphology And Hydrophobicity

Membrane synthesis is carried out by incorporating LDPE-HMDS/SiNPs into the PVDF membrane. Thermodynamic plays an important factor in the process of membrane synthesis, particularly in the mixing and de-mixing interaction of mixed components (PVDF polymer, NMP solvent, and LDPE-

HMDS/SiNPs). The addition of LDPE-HMDS/SiNPs may change the membrane structure, which in turn affects the wetting of the membrane when it comes in contact with amine absorbent during MGA operation. As shown in Figure 4 (left images), all synthesized composite membranes showed asymmetric structures. In essence, the PVDF membrane has an asymmetric structure and usually consists of several distinct layers. The cross-sectional membranes are composed of a sponge-like layer and a finger-like layer. Since water is the main proportion of the mixed-non-solvent in the coagulation bath, a visible cavity-like structure is formed due to the rapid liquid-liquid demixing. In addition, due to the presence of ethanol, the porous sponge-like structure can also be seen from the cross-sectional view in Figure 4 (left images).

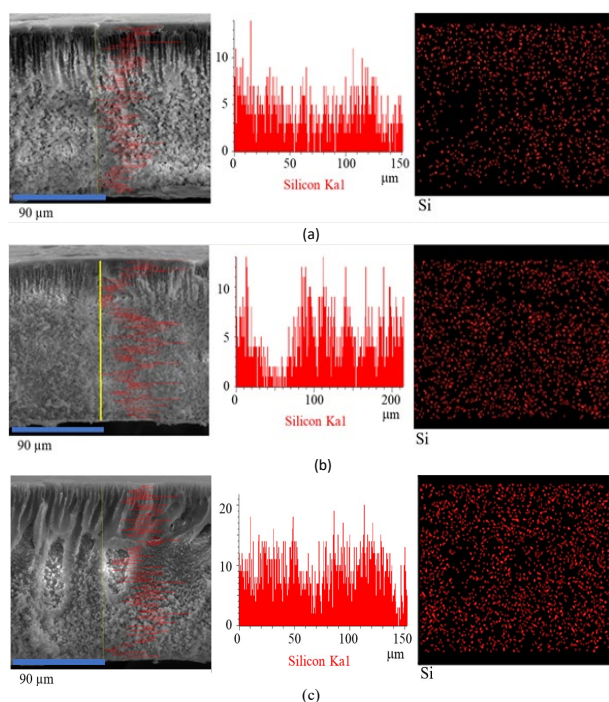


Figure 4 EDX lining (cross-section, left and center images) and mapping (surface, right image) of LDPE-HMDS/SiNPs-PVDF composite membranes with filler loading of (a) 1 wt.% (b) 3 wt.% (c) 5 wt.%

Interestingly, the cross-section of composite membrane loaded 3 wt.% LDPE-HMDS/SiNPs (Figure 4b, left image) shows that the finger-like length structure is shorter than the composite membrane loaded 1 wt.% loading LDPE-HMDS/SiNPs (Figure 4a, left image). The change in finger-like pore structures is due to the added LDPE-HMDS/SiNPs to the PVDF solution, which increases the membrane dope's viscosity. It causes a delay in the interdiffusion between the solvent in the polymer dope and the water/ethanol mixture in the coagulation bath, resulting in a smaller finger-like structure. The growth restriction of finger-like structures in 3 wt.% LDPE-HMDS/SiNPs is more severe than 1 wt.% LDPE-HMDS/SiNPs. The slow phase inversion process results in a lower membrane precipitation rate. Therefore, inhibiting the growth of finger-like structures. It is possible to form a sponge-like structure, which will reduce the membrane porosity. However, as shown in Figure 4c (left image), when LDPE-HMDS/SiNPs increase to 5 wt.%, it displayed more finger-like microvoids in the cross-section. It is contradicting to the earlier observation in 1 wt.% and 3 wt.% of

LDPE-HMDS/SiNPs composite membranes. This phenomenon may explain by the compatibility between organic polymers and inorganic fillers. As the concentration of inorganic fillers increases, it will produce colloidal instability, which will cause the particles to begin to agglomerate [23]. Therefore, it accelerates the phase separation during the phase inversion process. Two distinctive polymer layers will form, where the polymer-lean phase will tend to form large microcavities in the membrane structure. The microcavities will increase the surface pore size and porosity of the membrane [24]. However, at the same time, the surface tension of the membrane may decrease. Therefore, reducing the membrane's resistance to wetting.

The LDPE coating on HMDS/SiNPs not only enhances hydrophobicity. But, it also improves the compatibility between the organic PVDF membrane and inorganic LDPE-SiNPs nanofillers. Inorganic fillers tend to agglomerate within the polymer matrix because of the incompatibility between organic and inorganic materials. Filler aggregation becomes more critical at high concentrations of filler. Subsequently, there are interfacial defects, which affect the membrane function in the MGA process [25]. Therefore, it is crucial to improve the compatibility of the filler with the polymer matrix [26,27]. The LDPE-HMDS/SiNPs distribution via EDX lining (Figure 4, center image) and mapping (Figure 4, right image) were analyzed in order to verify the hypothesis that the LDPE coating on HMDS/SiNPs can improve compatibility with the PVDF membrane matrix. As shown in Figure 4, LDPE-HMDS/SiNPs uniformly distributed within the PVDF membrane, and there are no apparent aggregates of LDPE-HMDS/SiNPs. Under 1 wt.% LDPE-HMDS/SiNPs (Figure 4a, center image) and 3 wt.% LDPE-HMDS/SiNPs (Figure 4b, center image), some membrane regions are not covered by LDPE-HMDS/SiNPs and leave the membrane area blank. It may be because of insufficient LDPE-SiNPs added.

Further addition of LDPE-HMDS/SiNPs to 5 wt.% (Figure 4c, center image) will result in membrane cross-section covered by the LDPE-HMDS/SiNPs. Therefore, it exhibits higher EDX line intensity. Although as mentioned earlier, high concentrations of 5 wt.% LDPE-HMDS/SiNPs can cause particle agglomerations, EDX analysis still proves that LDPE-HMDS/SiNPs are well distributed in the PVDF membrane. These findings comply with the hypothesis. Good interaction between LDPE-HMDS/SiNPs and PVDF mainly due to the steric hindrance of LDPE coated on HMDS/SiNPs. The hydrophobic LDPE chain produces a spatial effect that hinders the coagulation of LDPE-HMDS/SiNPs. Therefore, fewer aggregates of LDPE-HMDS/SiNPs had observed in EDX mapping. LDPE-HMDS/SiNPs exhibit strong PVDF adhesion, thereby minimizing the agglomerates and interfacial void defects of LDPE-HMDS/SiNPs. Rosli *et al.*, (2019) also obtained similar results [17]. Nanofillers coated with LDPE have successfully prevented the aggregation of nanofiller in the membrane matrix.

This work also accesses the wettability of the composite membranes through static water contact angle measurement. A membrane with a high water contact angle value implies that it has a high resistance to wetting. According to the Wenzel model, the change in the water contact angle may attribute to the change in membrane surface roughness [28,29]. As the incorporation of LDPE-HMDS/SiNPs into the PVDF membrane has changed the membrane morphology. In Figure 5, the pristine PVDF and LDPE-HMDS/SiNPs-PVDF composite

membranes displayed comparable surface morphologies. Obviously, the pore size of the surface pores of the LDPE-HMDS/SiNPs-PVDF composite membranes are reduced because it is hardly visible in Figure 5b-5d. Whereas, for the pristine PVDF membrane, the pores are visible (Figure 5a). This reduction in pore size is mainly due to the delay in phase inversion process. As mentioned earlier, loading LDPE-HMDS/SiNPs into the PVDF solution will increase the viscosity of the membrane dope solution thereby reducing the precipitation rate of the membrane in the coagulation bath. As a consequent, the LDPE-HMDS/SiNPs-PVDF composite membrane has a smaller pore size. In addition, the incorporation of HMDS/SiNPs improves the surface roughness of the LDPE-HMDS/SiNPs-PVDF composite membrane, but the increment in roughness is not significant. Although the surface roughness of the LDPE-HMDS/SiNPs-PVDF composite membrane increases slightly, it also affects the water contact angle. As expected, all LDPE-HMDS/SiNPs-PVDF composite membranes displayed higher contact angles than the pristine PVDF membrane of 71.8° (Figure 5a) due to the changes of membrane morphology. Adding LDPE-HMDS/SiNPs at 5 wt.% displayed the highest contact angle of 111.8° (Figure 5d). This is because incorporating hydrophobic LDPE-HMDS/SiNPs into the polymer matrix had increase the surface roughness and reduce the pore size of the membranes which contributes to increase the water contact angle. At the same time, LDPE-HMDS/SiNPs also reduces the surface energy of the PVDF membrane, thereby reducing the adhesion of water to the surface of the membrane. Therefore, there is less contact between the water droplets and the membrane surface. Rezaei *et al.*, (2014) conducted a similar study in which the nano-scale hydrophobic montmorillonite (MMT) was incorporated into the PVDF membrane matrix. The hydrophobicity of the membrane increased from 80° to 99° [30]. Compared with the work of Rezaei *et al.*, (2014) the incorporation of hydrophobic LDPE-HMDS/SiNPs into the PVDF matrix showed a better improvement in membrane hydrophobicity [30]. Therefore, it is expected to exhibit better wetting resistance to maintain stable MGA long-term operation.

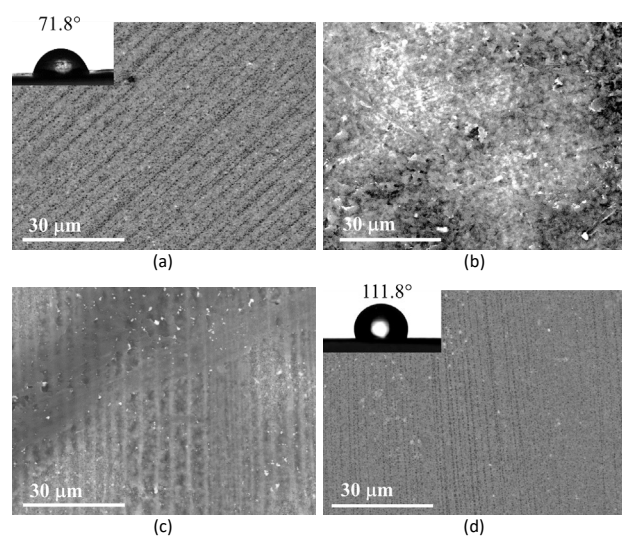


Figure 5 SEM images and water contact angle of LDPE-HMDS/SiNPs-PVDF composite membranes with filler loading of (a) 0 wt.% (pristine) (b) 1 wt.% (c) 3 wt.% and (d) 5 wt.%

3.3 Membrane Performance In MGA

The LDPE-HMDS/SiNPs-PVDF composite membranes and the pristine PVDF membrane were tested for MGA performance for comparison. In the present work, 1M MEA was used as an liquid absorbent. The addition of LDPE-HMDS/SiNPs successfully enhanced the membrane hydrophobicity, thereby reducing the penetration rate of MEA into the membrane pores. This promotes a lower mass transfer resistance and allows more CO₂ to flow across the composite porous membrane.

According to the MGA performance tests (Figure 6), the results showed that the CO₂ absorption flux of the LDPE-HMDS/SiNPs-PVDF (5 wt.%) composite membrane can achieve 2.4×10^{-3} mol/m².s. It is the highest among the composite membranes (1 wt.% and 3 wt.% of LDPE-HMDS/SiNPs), and the flux was twice that of the pristine PVDF membrane at 1.1×10^{-3} mol/m².s. This was attributed to the changed of membrane morphology when LDPE-HMDS/SiNPs was added to improve the hydrophobicity of the membrane. The membrane surface with improved hydrophobicity has a higher ability to prevent the MEA absorbent from entering the membrane pores. Therefore, improves the membrane stability during the long-term MGA operation. However, the pristine PVDF membrane was more susceptible to wet due to its low wetting resistance, as evidenced by the contact angle of 71.8°. This indicated that it is difficult for the pristine PVDF membrane to maintain its non-wetting state during the MGA process. Therefore, when the MEA absorbent invades the membrane pores, it will produce higher mass transfer resistance. As a result, the amount of CO₂ absorbed by the absorbent was reduced, resulting in a decrease in the flux of CO₂ absorption.

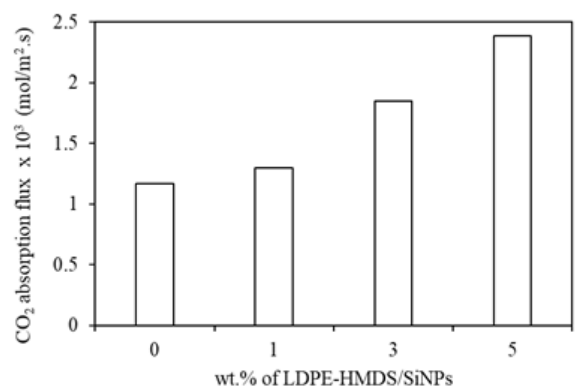


Figure 6 Average CO₂ absorption flux of pristine PVDF (0 wt.%) and LDPE-HMDS/SiNPs-PVDF composite membranes with LDPE-HMDS/SiNPs loading of 1-5 wt.% for 30 hours of MGA process

4.0 CONCLUSION

The improvement of membrane hydrophobicity is essential for the MGA process. It is to alleviate the pore wetting of the membrane. This work has successfully enhanced the hydrophobicity of pristine PVDF membrane by incorporating LDPE-HMDS/SiNPs into the membrane matrix. Because of the increase in the viscosity of the membrane dope, the addition of LDPE-HMDS/SiNPs alters the membrane morphology.

Therefore, leads to the possibility of forming a sponge-like structure. The hydrophobicity of the synthesized membranes has been enhanced with the addition of the LDPE-HMDS/SiNPs. As the concentration of LDPE-HMDS/SiNPs increased to 5 wt.%, the membrane hydrophobicity increased to a static contact angle of 111.8°. Such a high membrane hydrophobicity indicates that it has a strong resistance to wet. Therefore, in this work, the CO₂ absorption flux was shown increased by 2.4x10⁻³ mol/m².s, which was twice the pristine membrane. From this work, it can be clearly shown that coating HMDS/SiNPs with LDPE and then integrating them into the polymer matrix can improve the wetting resistance and MGA performance of the membrane. Due to its ability to inhibit liquid absorbents from entering the membrane pores, membrane with higher hydrophobicity are less likely to cause wetting.

Acknowledgement

This work was supported by the Fundamental Research Grant Scheme FRGS/1/2021/TKO/USM/02/8 (Account No: 203.PJKIMIA.6071513).

References

- [1] Wu, X., Zhao, B., Wang, L., Zhang, Z., Li, J., He, X., Zhang, H., Zhao, X., and Wang, H. 2018. Superhydrophobic PVDF membrane induced by hydrophobic SiO₂ nanoparticles and its use for CO₂ absorption. *Separation and Purification Technology*. 190: 108–116. DOI: <https://doi.org/10.1016/j.seppur.2017.07.076>
- [2] Lin, Y., Xu, Y., Loh, C. H., and Wang, R. 2018. Development of robust fluorinated TiO₂/PVDF composite hollow fiber membrane for CO₂ capture in gas-liquid membrane contactor. *Applied Surface Science*. 436: 670–681. DOI: <https://doi.org/10.1016/j.apsusc.2017.11.263>
- [3] Chang, P. T., Ng, Q. H., Ahmad, A. L., and Low, S. C. 2022. A critical review on the techno-economic analysis of membrane gas absorption for CO₂ capture. *Chemical Engineering Communications*. DOI: <https://doi.org/10.1080/00986445.2021.1977926>
- [4] Toh, M. J., Oh, P. C., Chew, T. L., and Ahmad, A. L. 2020. Preparation of polydimethylsiloxane-SiO₂/PVDF-HFP mixed matrix membrane of enhanced wetting resistance for membrane gas absorption. *Separation and Purification Technology*. 244: 116543. DOI: <https://doi.org/10.1016/j.seppur.2020.116543>
- [5] Chang, P. T., Baharuddin, I. M., Ng, Q. H., Teoh, G. H., Ahmad, A. L., and Low, S. C. 2022. Creating membrane-air-liquid interface through a rough hierarchy structure for membrane gas absorption to remove CO₂. *International Journal of Energy Research*. DOI: <https://doi.org/10.1002/er.7500>
- [6] Zhao, S., Feron, P. H. M., Deng, L., Favre, E., Chabanon, E., Yan, S., Hou, J., Chen, V., and Qi, H. 2016. Status and progress of membrane contactors in post-combustion carbon capture: A state-of-the-art review of new developments. *Journal of Membrane Science*. 511:180–206. DOI: <https://doi.org/10.1016/j.memsci.2016.03.051>
- [7] Siagian, U. W. R., Raksajati, A., Himma, N. F., Khoiruddin, K., and Wenten, I. G. 2019. Membrane-based carbon capture technologies: Membrane gas separation vs. membrane contactor. *Journal of Natural Gas Science and Engineering*. 67:172–195. DOI: <https://doi.org/10.1016/j.jngse.2019.04.008>
- [8] Himma, N. F., Wardani, A. K., and Wenten, I. G. 2017. The effects of non-solvent on surface morphology and hydrophobicity of dip-coated polypropylene membrane. *Materials Research Express*. 4(5): 054001. DOI: <https://doi.org/10.1088/2053-1591/aa6ee0>
- [9] Rosli, A., Ahmad, A. L., and Low, S. C. 2020. Functionalization of silica nanoparticles to reduce membrane swelling in CO₂ absorption process. *Journal of Chemical Technology & Biotechnology*. 95(4): 1073–1084. DOI: <https://doi.org/10.1002/jctb.6289>
- [10] Yan, S., Fang, M., Wang, Z., Xue, J., and Luo, Z. 2011. Economic analysis of CO₂ separation from coal-fired flue gas by chemical absorption and membrane absorption technologies in China. *Energy Procedia*. 4: 1878–1885. DOI: <https://doi.org/10.1016/j.egypro.2011.02.066>
- [11] Talavari, A., Ghanavati, B., Azimi, A., and Sayyahi, S. 2020. Preparation and characterization of PVDF-filled MWCNT hollow fiber mixed matrix membranes for gas absorption by Al₂O₃ nanofluid absorbent via gas-liquid membrane contactor. *Chemical Engineering Research and Design*. 156: 478–494. DOI: <https://doi.org/10.1016/j.cherd.2020.01.017>
- [12] Fashandi, H., Ghodsi, A., Saghafi, R., and Zarrebini, M. 2016. CO₂ absorption using gas-liquid membrane contactors made of highly porous poly(vinyl chloride) hollow fiber membranes. *International Journal of Greenhouse Gas Control*. 52: 13–23. DOI: <https://doi.org/10.1016/j.ijggc.2016.06.010>
- [13] Wu, X., Zhao, B., Wang, L., Zhang, Z., Zhang, H., Zhao, X., and Guo, X. 2016. Hydrophobic PVDF/graphene hybrid membrane for CO₂ absorption in membrane contactor. *Journal of Membrane Science*. 520: 120–129. DOI: <https://doi.org/10.1016/j.memsci.2016.07.025>
- [14] Chen, Z., Shen, Q., Gong, H., and Du, M. 2020. Preparation of a novel dual-layer polyvinylidene fluoride hollow fiber composite membrane with hydrophobic inner layer for carbon dioxide absorption in a membrane contactor. *Separation and Purification Technology*. 248: 117045. DOI: <https://doi.org/10.1016/j.seppur.2020.117045>
- [15] Lin, S-H., Tung, K-L., Chen, W-J., and Chang, H-W. 2009. Absorption of carbon dioxide by mixed piperazine-alkanolamine absorbent in a plasma-modified polypropylene hollow fiber contactor. *Journal of Membrane Science*. 333(1-2): 30–37. DOI: <https://doi.org/10.1016/j.memsci.2009.01.039>
- [16] Lin, Y-F., Ye, Q., Hsu, S-H., and Chung, T-W. 2016. Reusable fluorocarbon-modified electrospun PDMS/PVDF nanofibrous membranes with excellent CO₂ absorption performance. *Chemical Engineering Journal*. 284: 888–895. DOI: <https://doi.org/10.1016/j.cej.2015.09.063>
- [17] Rosli, A., Ahmad, A. L., and Low, S. C. 2019. Anti-wetting polyvinylidene fluoride membrane incorporated with hydrophobic polyethylene-functionalized-silica to improve CO₂ removal in membrane gas absorption. *Separation and Purification Technology*. 221: 275–285. DOI: <https://doi.org/10.1016/j.seppur.2019.03.094>
- [18] Nthunya, L. N., Gutierrez, L., Verliefe, A. R., and Mhlanga, S. D. 2019. Enhanced flux in direct contact membrane distillation using superhydrophobic PVDF nanofiber membranes embedded with organically modified SiO₂ nanoparticles. *Journal of Chemical Technology & Biotechnology*. 94(9): 2826–2837. DOI: <https://doi.org/10.1002/jctb.6104>
- [19] Sun, H., Xu, Y., Zhou, Y., Gao, W., Zhao, H., and Wang, W. 2017. Preparation of superhydrophobic nanocomposite fiber membranes by electrospinning poly(vinylidene fluoride)/silane coupling agent modified SiO₂ nanoparticles. *Journal of Applied Polymer Science*. 134(13): 44501. DOI: <https://doi.org/10.1002/app.44501>
- [20] Gharebbash, N., and Shakeri, A. 2015. Preparation and thermal and physical properties of nano-silica modified and unmodified. *Oriental Journal of Chemistry*. 31: 207–212. DOI: <https://doi.org/10.13005/oj/31.Special-Issue1.25>
- [21] Silverio, V., Canane, P. A. G., and Cardoso, S. 2019. Surface wettability and stability of chemically modified silicon, glass and polymeric surfaces via room temperature chemical vapor deposition. *Colloids and Surfaces A: Physicochemical and Engineering Aspects*. 570: 210–217. DOI: <https://doi.org/10.1016/j.colsurfa.2019.03.032>
- [22] Rosli, A., Ahmad, A. L., and Low, S. C. 2020. Enhancing membrane hydrophobicity using silica end-capped with organosilicon for CO₂ absorption in membrane contactor. *Separation and Purification Technology*. 251: 117429. DOI: <https://doi.org/10.1016/j.seppur.2020.117429>
- [23] Tan, P. C., Ooi, B. S., Ahmad, A. L., and Low, S. C. 2019. Formation of a defect-free polyimide/zeolitic imidazolate framework-8 composite membrane for gas separation: in-depth analysis of organic-inorganic compatibility. *Journal of Chemical Technology & Biotechnology*. 94(9): 2792–2804. DOI: <https://doi.org/10.1002/jctb.5908>

- [24] Bai, H., Zhou, Y., and Zhang, L. 2015. Morphology and Mechanical Properties of a New Nanocrystalline Cellulose/Polysulfone Composite Membrane. *Advances in Polymer Technology*. 34(1): 21471. DOI: <https://doi.org/10.1002/adv.21471>
- [25] Efome, J. E., Baghbanzadeh, M., Rana, D., Matsuura, T., and Lan, C. Q. 2015. Effects of superhydrophobic SiO₂ nanoparticles on the performance of PVDF flat sheet membranes for vacuum membrane distillation. *Desalination*. 373: 47–57. DOI: <https://doi.org/10.1016/j.desal.2015.07.002>
- [26] Luo, Z., Li, Y., Duan, C., and Wang, B. 2018. Fabrication of a superhydrophobic mesh based on PDMS/SiO₂ nanoparticles/PVDF microparticles/KH-550 by one-step dip-coating method. *RCS Advances*. 8(29): 16251–16259. DOI: <https://doi.org/10.1039/C8RA03262A>
- [27] Mistry, R. J., Saxena, M., Ray, P., and Singh, P. S. 2018. Octadecyl-silica—PVDF membrane of superior MD desalination performance. *Journal of Applied Polymer Science*. 135(13): 46043. DOI: <https://doi.org/10.1002/app.46043>
- [28] Barati Darband, Gh., Aliofkhaezai, M., Khorsand, S., Sokhanvar, S., and Kaboli, A. 2020. Science and Engineering of Superhydrophobic Surfaces: Review of Corrosion Resistance, Chemical and Mechanical Stability. *Arabian Journal of Chemistry*. 13(1): 1763–1802. DOI: <https://doi.org/10.1016/j.arabjc.2018.01.013>
- [29] Teoh, G. H., Chin, J. Y., Ooi, B. S., Jawad, Z. A., Leow, H. T. L., and Low, S. C. 2020. Superhydrophobic membrane with hierarchically 3D-microtexture to treat saline water by deploying membrane distillation. *Journal of Water Process Engineering*. 37: 101528. DOI: <https://doi.org/10.1016/j.jwpe.2020.101528>
- [30] Rezaei, M., Ismail, A. F., Hashemifard, S. A., and Matsuura, T. 2014. Preparation and characterization of PVDF-montmorillonite mixed matrix hollow fiber membrane for gas–liquid contacting process. *Chemical Engineering Research and Design*. 92(11): 2449–2460. DOI: <https://doi.org/10.1016/j.cherd.2014.02.019>